

Electrophoresis in colloidal dispersions in the counterion-dominated screening regime

Vladimir Lobaskin, Burkhard Dünweg, and Christian Holm

Max Planck Institute for Polymer Research, Ackermannweg 10, D-55128 Mainz, Germany

Martin Medeback, Thomas Palberg

Institut für Physik, Johannes Gutenberg-Universität, Staudingerweg 7, D-55128 Mainz, Germany

(Dated: Revised January 26, 2020)

We study the electrophoretic mobility of spherical charged colloids in a salt-free suspension as a function of the colloidal concentration. Using an effective reduced electrokinetic (zeta) potential and a suitable reduced screening parameter we are able to map experimental data onto numerical simulations of model colloids that were constructed to have the same reduced zeta potential. We observe two different volume fraction-dependent regimes for the electrophoretic mobility, that can be explained in terms of the ionic double layer, and its relation to the dynamical effective charge. We show that this concentration dependence can be parameterized with the effective zeta potential and, even in the absence of added salt, with an effective screening length.

PACS numbers: 82.45.+z, 82.70.Dd, 66.10.-x, 66.20.+d

The current understanding of electrokinetic and electro-rheological phenomena in colloidal systems is based on a central quantity, the electrokinetic potential or zeta (ζ) potential, which is decisive for e. g. the electrophoretic motion of the particles, the overall flow behavior of the dispersion, electroosmosis along surfaces, sedimentation, and coagulation [1, 2, 3, 4, 5]. For the simplest case, an isolated colloidal sphere with radius R and charge Ze (where e denotes the elementary charge) in a solvent of viscosity η and dielectric constant

(Hückel limit), Stokes' law implies that the drift velocity v in a weak external electric field E is given by $v = ZeE/(6\eta R)$, and hence the electrophoretic mobility, defined as $\mu = v/(eE)$, is given by $\mu = 2\eta/(3eR)$, where $\phi = Ze/(4\pi\eta R)$ is the electrostatic potential at the surface of the sphere. As the ionic double layer is absent, the electrokinetic potential has to be determined at the same surface as the electrostatic one and is therefore identical to the latter. The mobility μ . Furthermore, mobility data yield neither Z nor R , but only the ratio $Z=R$.

In the more general interacting case (finite concentration of colloids, counterions, and/or salt), (i) no longer coincides with the surface electrostatic potential, and (ii) the relation between ϕ and μ is more complicated. The reason for (i) is that a highly charged sphere is covered with a "stem" layer of counterions which are so tightly coupled to its motion that a description in terms of hydrodynamics with solvent viscosity η will fail in this region. For the combined sphere-layer system, one therefore introduces an effective sphere with increased radius R_{eff} and decreased charge Z_{eff} , with $\phi = Z_{\text{eff}}e/(4\pi\eta R_{\text{eff}})$. For solving the electrostatic problem, this splitting of the ion cloud into a "free" and a "condensed" part is done within the framework of charge renormalization theory [6]. The reason for (ii) is that electrophoresis at finite concentration is a complicated

many-body problem and the Stokes formula does not hold even for the effective spheres [1, 2, 3, 4, 5].

Apart from the Hückel limit of vanishing concentration, there is however yet another case where single-sphere theories are applicable. If each sphere is surrounded by a well-defined localized ion cloud (the double layer), then both electrostatic and hydrodynamic interactions are screened beyond the length scale of this layer | note that the electric net force on the system "sphere plus cloud" is zero, due to charge neutrality, and hence does not give rise to large-scale hydrodynamic flow [7, 8]. Even such a single-sphere problem is quite challenging, due to the non-trivial influence of the ion motion [9, 10, 11, 12].

Strictly spoken, a localized double layer occurs only in the case of sufficiently large salt concentration, where the thickness $l_b = \frac{1}{D} \sqrt{\frac{2}{\phi}} \eta$ is, for monovalent salt, given by the Debye formula $D = 4\pi l_b n_{\text{salt}}$, where n_{salt} is the number density of salt ions, and l_b the Bjerrum length, $l_b = e^2/(4\pi k_B T)$, k_B and T denoting Boltzmann's constant and the temperature, respectively. Essentially all theories (including recent work treating effects of double layer overlap [13]) deal with this case. Typically [11], the result of a single-sphere consideration is a relation between three dimensionless quantities: The reduced mobility $\mu_{\text{red}} = 6\eta l_b$, the reduced zeta potential $\zeta_{\text{red}} = e/(k_B T)$, and the reduced screening parameter R_{eff} . In the Hückel limit $R_{\text{eff}} = 0$ one simply has $\mu_{\text{red}} = \zeta_{\text{red}}^2$.

The present Letter focuses on the situation where the salt concentration is very low or even zero, while the colloidal concentration is finite. For this case no quantitative first-principles theory exists. We compare the results of computer simulations with experimental data and show that a quite favorable agreement can be obtained if the comparison is done in terms of reduced parameters even if the "bare" parameters differ substantially. These re-

sults are obtained in a regime where the ion cloud overlap is not yet very strong. Furthermore, we show that in this regime the effect of finite colloid concentration can be reduced to a modification of the screening parameter (account for the finite electrolyte concentration).

In order to elucidate our approach, let us again consider the single colloid case with salt. We first note that a theory which writes μ_{red} as a function of just two dimensionless variables (R_{eff} , μ_{red}) can only be approximate. This follows directly from a dimensional analysis of the problem: The original physical parameters on which can depend are (i) the solvent properties $k_B T$ and ρ ; (ii) the charge cloud properties n , D_+ and D_- (the mobilities of the positive and negative salt ions, respectively); and (iii) the colloid properties R_{eff} and Z_{eff} . This seven-variable set we can transform to an equivalent set comprising the seven variables $l_B = R_{\text{eff}}$, $\sigma_0 = (6 l_B)^{1/3}$, l_B , $D_{+/-} = D_{+/-} = (\rho k_B T)$, R_{eff} and μ_{red} . Of these, only the second and the third are not dimensionless, supplying the natural units for time and length. As μ_{red} is dimensionless, it cannot depend on these two variables. However, the dependence on the remaining five dimensionless parameters remains. A two-parameter theory therefore essentially means to ignore the dependence on the three scaling variables $l_B = R_{\text{eff}}$, $D_{+/-}$. However, this is reasonable for typical experimental systems where the colloid size is much larger than the Debye length, and $D_{+/-}$ do not vary strongly (and are of order unity [5]).

For the low salt case we may apply a quite analogous scaling analysis. This becomes most transparent if we consider the case we have treated in our simulations, which is a single charged colloid with its counterions confined to a finite box with periodic boundary conditions. The six input parameters are now $k_B T$ and R_{eff} , Z_{eff} , the collective diffusion coefficient of the counterions D , and the linear system size L . The latter may be re-written in terms of the counterion density $n = Z_{\text{eff}}/L^3$. Again we transform to new variables $l_B = R_{\text{eff}}$, σ_0 , l_B , $D' = D = (\rho k_B T)$, R_{eff} and μ_{red} , where we have defined $\sigma_0^2 = 4 l_B n$ and $l_B = \sigma_0^{-1}$. It should be emphasized that this is a mere re-parametrization, without (at the present stage) implying any statements about the validity of a linearized Poisson-Boltzmann equation, presence of screening, etc.. Applying the same dimensionality considerations as above, and again ignoring the dependence on $l_B = R_{\text{eff}}$ and D' , one finds that μ_{red} should depend on R_{eff} and μ_{red} , such that simulations and experiments should yield the same μ_{red} value if their physical situations are identical in terms of these two parameters. It should be noted that this is expected to be only true for a sufficiently localized charge cloud which does not strongly overlap with that of the periodic image, such that the difference between the periodic "crystal" of the simulation and the disordered arrangement of colloids in the experiment does not matter. In what follows, we will

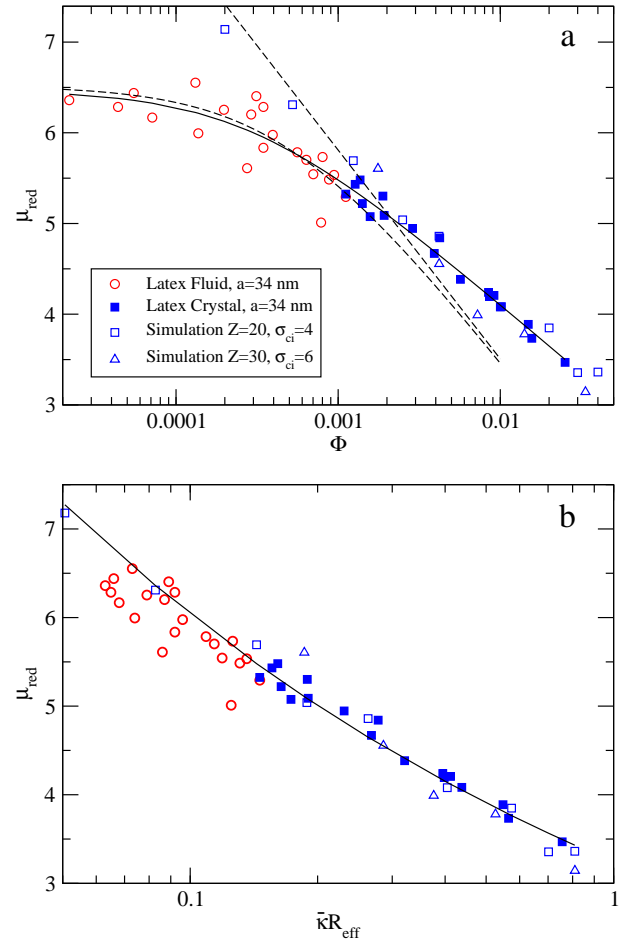


FIG. 1: Magnitude of electrophoretic mobility of a spherical particle as a function of the particle volume fraction (a), and of the reduced screening parameter (b). The screening parameter was calculated based upon counterion and salt contributions as explained in the text. The dashed curves are the result of a Hückel-type calculation $\mu_{\text{red}} = \ln(l_B Z_{\text{eff}}/(R_{\text{eff}}^3 \sigma_0^2)) = \ln(1/(3 + 3n_{\text{salt}}/(n Z_{\text{eff}})))$, where we supposed the salt concentration to be 2 M (see text for the further explanation). The solid curves represent the fit to the experimental dataset.

report our results which confirm that this is indeed the case. We would like to stress that we consider this a non-trivial result, since (i) the (ignored) value of $l_B = R_{\text{eff}}$ is substantially larger for the simulation than for the experiment, and (ii) the comparison has to be done in terms of effective parameters R_{eff} and Z_{eff} , whose determination is far from straightforward and obvious.

Our computer model is composed of small counterions, plus one large charged sphere which is built by wrapping a network of small particles around a large sphere. All particles are coupled dissipatively to a Lattice Boltzmann (LB) background [14, 15] which provides the hydrodynamic interactions. Thermal motion is taken into account via Langevin noise, and electrostatic interactions are calculated via the Ewald summation technique [16].

In our unit system, we use $l_B = 1.3$, $R = 3$ or 5 and $Z = 20, 30$, or 60 , while the small monovalent ions have radius unity, which is also the LB lattice spacing. To distinguish the friction produced by the colloidal sphere itself and the friction coming from the ions, the nearest colloid-ion distance was set to $r_{ci} = R + 1$. For further details, see Refs. [17, 18]. The electrophoretic mobility was obtained by applying an external electric field, and averaging the steady-state velocity of the colloidal particle. For some data points, we checked that the simulation was indeed in the linear regime, by comparison with data which we obtained in thermodynamic equilibrium via Green-Kubo integration.

The experimental system comprises thoroughly deionized aqueous suspensions of latex spheres (lab code PnBAPS68, kindly provided by BASF, Ludwigshafen, Germany) with diameter $2R = 68\text{ nm}$, low polydispersity and high charge (bare charge $Z = 1500$; effective charge from conductivity $Z = 450$ [19, 20]). They show a low lying and narrow first order freezing transition at a particle number density of $n_F = (6.1 \pm 0.3) \text{ m}^{-3}$. Due to the small size optical investigations are possible without multiple scattering up to large n . Using Doppler velocimetry in the super-heterodyning mode [21] we here studied the electrophoretic mobility in the range of $0.1 \text{ m}^{-3} \leq n \leq 160 \text{ m}^{-3}$, corresponding to volume fractions $\phi = (4/3)R^3 n$ of $5 \times 10^{-4} \leq \phi \leq 2.5 \times 10^{-2}$ [22]. Consistent with data taken on other species and also at elevated salt concentrations [23], the mobility as shown in Fig. 1 shows a plateau at low ϕ and descents fairly linearly in this semi-logarithmic plot at larger ϕ . The particle charges in the simulation were chosen to match the reduced electrokinetic potentials $\zeta_{red} = 8.5$ for PnBAPS68 particles, which were obtained numerically based on the charge renormalization concept [6] using the Poisson-Boltzmann cell model [20, 24]. The pairs of parameters $Z = 20; R = 3$, and $Z = 30; R = 5$ correspond roughly to this value of ζ_{red} .

Comparing the experimental and simulation data in Fig. 1 (a), where ζ_{red} is shown as a function of ϕ , one sees that the agreement is quite good. This is not too surprising, since ϕ can be viewed as another dimensionless variable (instead of R_{eff}) which parametrizes the counterion density. However, simulation and experiment deviate in the regime of very low volume fractions. The reason is that for very small ϕ the dissociation of water starts to play a role | the size of the counterion cloud is no longer determined by the colloid-colloid distance, but rather by the salt concentration, and the unscreened Huckel limit is never reached. From dimensional analysis, we only know that this should give rise to yet another scaling variable $\sim R_{eff}$, where $\sim^2 = 4 l_B n_{salt}$. However, from the arguments put forward in Ref. [6], we conclude that these two should be approximately combined to one single scaling variable R_{eff} with $\sim^2 = 4 l_B (n + n_{salt})$. Essentially, the argument is that the electrostatic poten-

tial in the regions centered between the colloids should vary only weakly, such that a description in terms of a linearized Poisson-Boltzmann equation is possible, where the screening is given by the local ion concentrations in these regions. In a simple approximation, we replace the latter by the mean sample concentrations, giving rise to . Figure 1 (b) shows that this strategy to include the effect of salt is indeed successful.

Let us try to understand the observed mobility decrease with the concentration. Except for the distance between colloids, the properties of the ionic double layer change with the volume fraction. The dilution leads to a decrease of number of counterions in the vicinity of the colloidal surface. The effect on the mobility is, in principle, two-fold. At a very low concentrations, the dilution leads to evaporation of the Stern layer, as for the system with charge $Z = 60$ on Fig. 2 and, hence, to variation of the potential. Secondly, the dilution of the diffuse double layer leads to reduction of ionic contribution to the colloidal mobility. The number of contributing ions is, obviously, controlled by the electrostatic correlation length (\sim^1). Therefore, in this region one can expect that the reduced mobility is completely defined by the electrostatic properties. One can use the static charge renormalization procedure [6] to estimate the mobility. Basing on the results of a variational Poisson-Boltzmann approach [25], we expect that the reduced surface potential (according to the static criteria) at $R = 1$ changes as $\zeta_{eff} = k_B T = \ln(l_B Z_{eff} / (R_{eff}^3 \sim^2))$, from which, using our definition of the screening constant \sim , we get in the Huckel limit $\zeta_{red} = \ln(1/(3 + 3n_{salt} / (n Z_{eff})))$. It is interesting to note that in the counterion dominated screening regime, the particle volume fraction (calculated with the hydrodynamic radius R_{eff}) becomes the only parameter controlling the reduced mobility, provided that the screening is described by . The reduced mobilities following from the scaling relations above are shown in Fig. 1 (dashed curves). They predict reasonable values for the simulated and experimental systems at low concentrations, as expected.

Figure 2 shows the same simulation data as those of Fig. 1, augmented by an additional data set obtained at $Z = 60$. Here the charge is strong enough such that $R_{eff} = 4 > R = 3$ and $Z_{eff} = 30 < Z$, giving rise to a reduced zeta potential $\zeta_{red} = 10$. These values pertain to the value $\phi = 0.01$. In this high-concentration regime, the zeta potential is approximately constant, and roughly coincides with that of the $Z = 20, Z = 30$ systems. Hence, the ζ_{red} values are very similar, and here the mobility decreases roughly logarithmically with ϕ (as do the experimental data). However, in the regime of further dilution, ζ_{red} increases sharply. This is due to the fact that now the Stern layer evaporates, i.e. Z_{eff} increases. In this regime, we find empirically ζ_{red} / \sim^1 . Ultimately, at $\phi = 0$ one would reach the Huckel limit value $\zeta_{red} = \zeta_{red} = 26$.

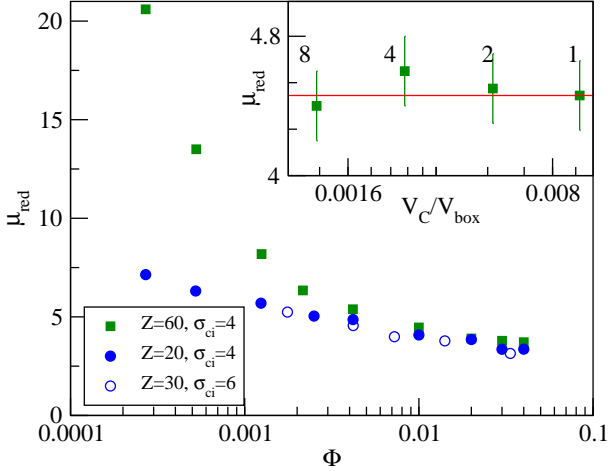


FIG. 2: Electrophoretic mobility of a spherical particle of the indicated charge and size as a function of the particle volume fraction in a salt-free system. The inset shows the mobility of the particle of $Z = 60$ as a function of $V_c = V_{\text{box}}$, where V_c is the volume of one colloidal particle, and V_{box} is the system volume. Here the number of particles (indicated in the figure) was chosen such that the volume fraction is constant.

To assess the electrokinetic relevance of the reduced parameters defined above, let us look at the structure of the ionic double layer of a moving colloidal particle (Fig. 3). The position of the "shear plane", which discriminates between "free" and "condensed" ions, can be inferred from the ion velocity distribution around the colloidal particle. We looked at the normalized velocity cross-correlation function $\langle \mathbf{v}_i \cdot \mathbf{v}_c \rangle = \langle \mathbf{v}_c^2 \rangle - 1$ at zero field. Here \mathbf{v}_i denotes the velocity of an ion, \mathbf{v}_c the colloid velocity. Since the instantaneous value is of course zero, we replaced \mathbf{v}_i and \mathbf{v}_c by their respective time-averaged values, where we measured over a time interval of 500 in our unit system [26].

The cross-section of the correlation function profile has a clear structure: A plateau of $\langle \mathbf{v}_i \cdot \mathbf{v}_c \rangle = \langle \mathbf{v}_c^2 \rangle - 1$ and two decay wings on both sides of the particle. The plateau is formed by the ions that move with the colloidal sphere and spans till the radius of the colloid coated with a ionic monolayer, i.e. roughly to σ_{ci} . We now define the position of the shear plane via extrapolation of the wings to $\langle \mathbf{v}_i \cdot \mathbf{v}_c \rangle = \langle \mathbf{v}_c^2 \rangle - 1 = 1$. This distance from the colloid center therefore defines the effective hydrodynamic radius of the colloid R_{eff} . The average charge within this radius (consisting of colloid charge and bound counterions) corresponds to the "dynamical" effective charge Z_{eff} , and these two values together define the potential. It should be noted that the systems $Z = 20$ and $Z = 30$ are so weakly charged that the effective parameters are very close to the bare parameters.

Finally, we would like to note that the mapping of finite volume fraction system onto a single particle theory can be also justified. For this we consider a set of

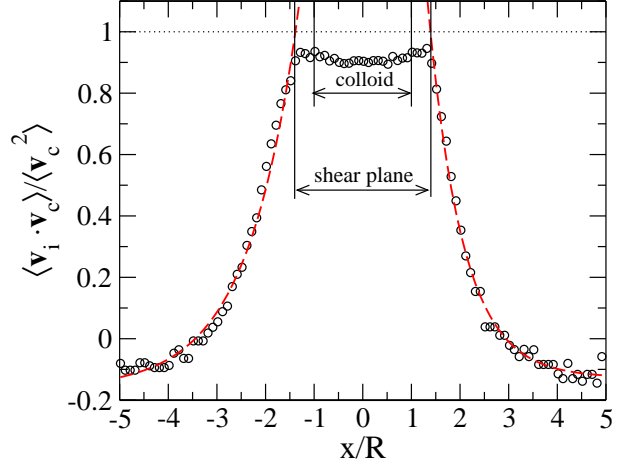


FIG. 3: A cross-section of the velocity cross-correlation function $\langle \mathbf{v}_i \cdot \mathbf{v}_c \rangle = \langle \mathbf{v}_c^2 \rangle - 1$ without electric field for a particle of charge $Z = 120$ at volume fraction $\Phi = 0.01$. The wings of the distribution were fitted by an exponential function $y = A \exp(-r/B) + C$ (dashed curves). The extrapolation of the fitting curve to the value 1 defines the shear plane position, the effective hydrodynamic radius of the colloid, and the potential.

systems (in a simulation) with primary cells of different sizes containing an appropriate number of particles, so that the particle volume fraction remains fixed. Increasing the number of particles in the main cell then corresponds to a gradual transition from the symmetry of a cubic crystal to an isotropic liquid (as it would be observed in a bulk simulation [27]). The simulation results (see inset in Fig. 2) show that, within our numerical resolution, the mobility is not affected by the positions of the nearest neighbors. One can hence assume that hydrodynamic interactions between the periodic images are strongly screened. This is expected for a reasonably well-defined double layer [7, 8], and corroborates the general effective single-particle picture, according to which the mobility is governed by the shear stresses within that layer. Quite analogous to the absence of finite-size effects in the simulations is the experimental observation that Φ is remarkably smooth at the freezing transition (see Fig. 1). Electrophoretic data on other particles as well as conductivity data show similar behavior [19, 24].

In summary, we have studied the behaviour of electrophoretic mobility of colloidal particle in the counterion-dominated screening regime, which can be observed at finite particle volume fractions and low electrolyte strengths. Basing on the idea of charge renormalization similar to what is used for electrostatic problems, we suggest a set of effective control parameters, the reduced potential $\mu_{\text{red}} = k_B T_{\text{eff}}/R_{\text{eff}}$ and screening constant σ_{ci} , controlling the static and dynamical properties of the system. Moreover, in a dilute regime these values can be combined in such a way that the particle volume

fraction becomes the only control parameter of the problem. Our model is supported by a successful matching of the LB/MD computer simulations of the primitive model electrolyte and Laser Doppler velocimetry measurements with similar reduced and R , whose non-rescaled system parameters differ from each other by more than an order of magnitude. We argue that with these reduced parameters, one can map the electrokinetic problem at finite concentration onto a standard electrokinetic model of a single particle in an electrolyte bath.

We thank J. Horbach, O. V. Vinogradova and F. Carrigue for stimulating discussions. This work was funded by the SFB TR 6 of the Deutsche Forschungsgemeinschaft.

[1] M. von Smoluchowski, *Bull. Acad. Sci. Cracovie, Classe Sci. Math. Natur.* 1, 182 (1903).
 [2] E. Huckel, *Physik. Z.* 25, 204 (1924).
 [3] S. S. Dukhin and B. V. Derjaguin, in *Surface and Colloid Science* vol. 7, edited by E. Matijevic (John Wiley, New York, 1974).
 [4] R. J. Hunter, *Zeta Potential in Colloid Science* (Academic Press, London, 1981).
 [5] W. B. Russel, D. A. Saville, and W. R. Schowalter, *Colloidal Dispersions* (Cambridge University Press, Cambridge, 1989).
 [6] S. Alexander, P. M. Chaikin, P. G. de Gennes, G. J. Morales, P. Pincus, and D. Hone, *J. Chem. Phys.* 80, 5776 (1984).
 [7] D. Long and A. A. Jilgari, *Eur. Phys. J. E* 4, 29 (2001).
 [8] M. Tanaka and A. Y. Grosberg, *J. Chem. Phys.* 115, 567 (2001).
 [9] D. C. Henry, *Proc. R. Soc. (London) Ser. A* 133, 106 (1931).
 [10] P. H. Wiersemann, A. L. Loeb, and J. T. G. Overbeek, *J. Colloid Interface Sci.* 22, 70 (1966).
 [11] R. O'Brien and L. Whiite, *J. Chem. Soc. Faraday Trans.* 74, 1607 (1978).
 [12] M. Lozada-Cassou and E. Gonzales-Tovar, *J. Colloid Interface Sci.* 239, 285 (2001).
 [13] F. Carrigue, F. J. Amayo, M. L. Jimenez, and A. V. Delgado, *J. Phys. Chem. B* 107, 3199 (2003).
 [14] P. Ahlrichs and B. D. Dunweg, *Int. J. Mod. Phys. C* 9, 1429 (1998).
 [15] P. Ahlrichs and B. D. Dunweg, *J. Chem. Phys.* 111, 8225 (1999).
 [16] M. A. Allen and D. J. Tildesley, *Computer Simulation of Liquids* (Oxford University Press, 1987).
 [17] V. Lobaskin and B. D. Dunweg, *New J. Phys.* 6, 54 (2004).
 [18] V. Lobaskin, B. D. Dunweg, and C. Holm, *J. Phys. Condens. Matter* 16, S4063 (2004).
 [19] P. Wetet, H.-J. Schope, and T. Palberg, *J. Chem. Phys.* 116, 10981 (2002).
 [20] L. Shapran, M. M. Edebach, P. Wetet, H.-J. Schope, T. Palberg, J. Horbach, T. Kerner, and A. Chaterji, *Colloid Surf. A* XXX, in press (2005).
 [21] M. M. Edebach and T. Palberg, *J. Chem. Phys.* 119, 3360 (2003).
 [22] M. M. Edebach and T. Palberg, *J. Phys. Condens. Matter* 16, 5653 (2004).
 [23] T. Palberg, M. M. Edebach, N. Garbow, M. Evers, A. B. Fontecha, and H. Reiber, *J. Phys. Condens. Matter* 16, S4039 (2004).
 [24] M. M. Edebach, R. Chulia-Jordan, H. Reiber, H.-J. Schope, R. Biehl, M. Evers, D. Hessinger, J. Olah, T. Palberg, E. Schonberger, et al., *J. Chem. Phys.* 123, in press (2005).
 [25] R. R. Netz and H. Orlund, *Eur. Phys. J. E* 11, 301 (2003).
 [26] B. J. Alder and T. E. Wainwright, *Phys. Rev. A* 1, 18 (1970).
 [27] V. Lobaskin and P. Linse, *J. Chem. Phys.* 111, 4300 (1999).